Activation Loop Phosphorylation Modulates Bruton's Tyrosine Kinase (Btk) Kinase Domain Activity

Laura Lin,*,‡ Robert Czerwinski,§ Kerry Kelleher,‡ Marshall M. Siegel,|| Paul Wu,⊥ Ron Kriz,‡ Ann Aulabaugh,§ and Mark Stahl‡

Structural Biology and Computational Chemistry, Enzymology and Biophysical Characterization, Chemical Technologies, Chemical and Screening Sciences, and Inflammation, Wyeth Research, 200 Cambridge Park Drive, Cambridge, Massachusetts 02140

Received October 22, 2008; Revised Manuscript Received January 12, 2009

ABSTRACT: Bruton's tyrosine kinase (Btk) plays a central role in signal transduction pathways regulating survival, activation, proliferation, and differentiation of B-lineage lymphoid cells. A number of cell signaling studies clearly show that Btk is activated by Lyn, a Src family kinase, through phosphorylation on activation loop tyrosine 551 (Y^{551}). However, the detailed molecular mechanism regulating Btk activation remains unclear. In particular, we do not fully understand the correlation of kinase activity with Y^{551} phosphorylation, and the role of the noncatalytic domains of Btk in the activation process. Insect cell expressed full-length Btk is enzymatically active, but a truncated version of Btk, composed of only the kinase catalytic domain, is largely inactive. Further characterization of both forms of Btk by mass spectrometry showed partial phosphorylation of Y^{551} of the full-length enzyme and none of the truncated kinase domain. To determine whether the lack of activity of the kinase domain was due to the absence of Y^{551} phosphorylation, we developed an in vitro method to generate Y^{551} monophosphorylated Btk kinase domain fragment using the Src family kinase Lyn. Detailed kinetic analyses demonstrated that the in vitro phosphorylated Btk kinase domain has a similar activity as the full-length enzyme while the unphosphorylated kinase domain has a very low k_{cat} and is largely inactive. A divalent magnesium metal dependence study established that Btk requires a second magnesium ion for activity. Furthermore, our analysis revealed significant differences in the second metal-binding site among the kinase domain and the full-length enzyme that likely account for the difference in their catalytic profile. Taken together, our study provides important mechanistic insights into Btk kinase activity and phosphorylation-mediated regulation.

The human kinome is composed of 518 protein kinases (*1*), among which protein tyrosine kinases (PTKs)[1] form the largest family (*2*). PTKs are important regulators of signal transduction pathways that mediate many cellular processes including transcription, metabolism, cell cycle progression, apoptosis, and differentiation. Bruton's tyrosine kinase (Btk) belongs to the Tec family nonreceptor PTKs that include Tec, Itk, Bmx, and Txk. Btk is expressed in B cells and myeloid cells but not in T cells and is downregulated in plasma cells. Mutations in the gene encoding human Btk result in X-linked agammaglobulinemia (XLA) (*3*−*5*). XLA is one of the most frequently inherited immunodeficiency diseases in man and is characterized by an almost complete arrest of B-cell differentiation at the pre-B-cell stage. A spontaneous point mutation in murine Btk (R28C) results in a milder condition in mice termed X-linked immunodeficiency (xid) (*6, 7*). Btk is intimately involved in a number of signaling pathways regulating survival, activation, proliferation, and differentiation of B-lineage lymphoid cells (*8*). Specifically, upon B-cell antigen receptor (BCR) engagement, phosphatidylinositol 3-kinase and the Src family kinase Lyn are activated. Btk is then recruited to the plasma membrane through interactions between Btk pleckstrin homology (PH) domain and phosphatidylinositol 3,4,5-trisphosphate. Btk is activated initially through phosphorylation by Lyn at the activation loop tyrosine 551 (Y^{551}), followed by autophosphorylation on tyrosine 223 (Y^{223}) in the SH3 domain (*9*−*14*). Activated Btk then phosphorylates and activates phospholipase-Cγ leading to several important downstream events including calcium ion transport, NF-*k*B activation, proliferation, and ultimately autoantibody production (*3, 15*). Therapies targeting B cells for depletion, such as the anti-CD20 antibody Rituxan, have proven to be effective in the treatment of rheumatoid arthritis and non-Hodgkin's lymphoma. Blocking B lymphocyte function with Btk antagonists represents an attractive opportunity to treat diverse diseases such as inflammations, asthma, and malignances.

Btk shares significant structural and sequence homology with other members of the Tec family kinases. Btk is a multidomain protein composed of an N-terminal pleckstrin homology (PH) domain, a proline-rich Tec homology region,

* To whom correspondence should be addressed. Telephone: (617) 665-5033. Fax: (617) 665-5386. E-mail: lllin@wyeth.com.
‡ Structural Biology and Computational Chemistry.
§ Enzymology and Biophysical Characterization.
|| Chemical Technologies, Chemical and Screening Sciences.
⊥ Inflammation.

[1] Abbreviations: PTK, protein tyrosine kinase; Btk, Bruton's tyrosine kinase; Itk, interleukin-2 tyrosine kinase; SH3, Src homology domain 3; SH2, Src homology domain 2; Csk, C-terminal Src kinase.

10.1021/bi8019756 CCC: $40.75
Published on Web 02/10/2009

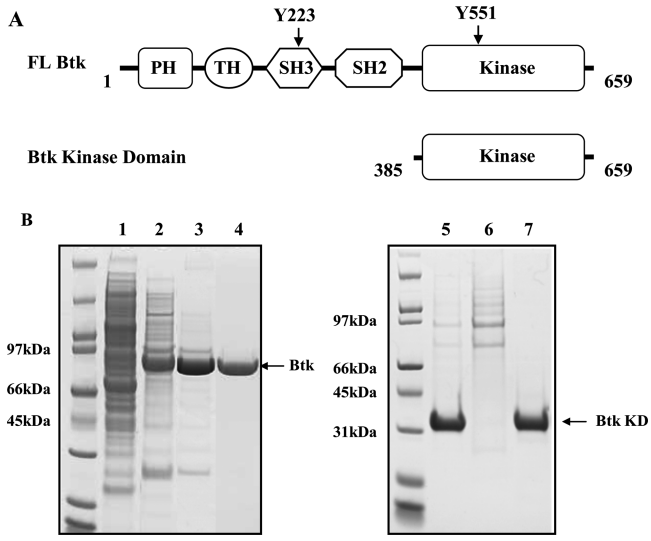

FIGURE 1: (A) Schematic drawing of full-length Btk protein domain arrangement and the kinase domain truncation used in this study. (B) Purification of full-length Btk and its kinase domain. Samples were separated on a 10−20% SDS-PAGE and revealed by Coomassie Blue staining. Lanes 1−4: full-length Btk. Lane 1, total soluble lysate; lane 2, Ni column elution; lane 3, HQ anion exchange column; lane 4, size exclusion chromotography. Lanes 5−7: Btk kinase domain. Lane 5, Ni elution; lane 6, flowthrough of HS cation-exchange column (contaminant removal); lane 7, HQ column elution.

an SH3 domain, SH2 domain, and a C-terminal catalytic kinase domain (*16, 17*) (Figure 1A). The three-dimensional structures of the individual Btk domains have been determined and have provided a structural based understanding of their various cellular functions such as pathway activation and signaling (*18*−*21*). However, the detailed molecular mechanisms regulating Btk activation remain poorly understood in part due to the lack of full-length or multidomain Btk structures, and the correlation of kinase activity with its phosphorylation state. X-ray synchrotron radiation scattering analysis indicated that, in solution, Btk exists most likely in an extended conformation with little or no interdomain interactions which suggests a different domain−domain regulatory mechanism when compared with the closely related Src family kinases (*22*).

Like many protein kinases, phosphorylation is a critical regulatory mechanism for controlling Btk function. In addition to the activation loop Y^{551} and SH3 autophosphorylation site Y^{223}, there have been reports of Btk phosphorylation on S^{180} by PKCβ (*23*) and of Y^{617} autophosphorylation that downregulates Btk function (*24*). Btk kinase activity is widely believed to correlate with the extent of Y^{551} phosphorylation (*13, 14, 25*). When overexpressed in *Spodoptera frugiperda* cells, FL-Btk is phosphorylated on a number of different residues including Y^{551}. The kinase dead K430R mutant enzyme, however, lacked a majority of these phosphorylation sites, indicating these sites were the consequence of autocatalytic activity (*22*). Furthermore, overexpression of the Btk kinase domain results in an unphosphorylated protein (*20*) that leads us to believe that the domains outside of the kinase domain region could potentially play a positive regulatory role in Btk autoactivation process.

To understand the relationship between Btk phosphorylation and kinase activity, we have generated a homogeneous, in vitro phosphorylated Btk kinase domain fragment using the upstream activating kinase Lyn. The protein was shown to be monophosphorylated, and the phosphorylation site was mapped to the activation loop residue Y^{551}. Detailed kinetic analysis was carried out on the phosphorylated kinase domain (pKD), its unphosphorylated counterpart (KD), and the full-length Btk enzyme, to compare the catalytic constants and kinetic mechanism. Furthermore, we established that Btk requires a second divalent metal ion for activity. Our study demonstrated that the unphosphorylated Btk kinase domain is mostly inactive. However, a single activation loop phosphorylation can restore its full catalytic activity when compared to the full-length enzyme. Specifically, steady-state kinetic analysis illustrated that Y^{551} phosphorylation led to a significant increase in the reaction k_{cat} for Btk kinase domain while the K_m for either ATP or two of the peptide substrates remained mostly unchanged. A divalent magnesium metal dependence study established that, while the full-length Btk binds to the second metal ion (M2) with a low mM affinity, the apparent K_m of the kinase domain for the M2-binding site was significantly elevated. Y^{551} phosphorylation reversed this K_m increase by more than 3-fold, implying that the residues involved in the M2-binding site contributed, at least in part, to the low activity of the kinase domain. Interestingly, our studies also suggest a positive regulatory role for the noncatalytic domains of Btk.

EXPERIMENTAL PROCEDURES

Protein Expression and Purification. Full-length human Btk and a kinase domain construct that encodes Btk residues P385-S659 were overexpressed using Baculovirus and *Spodoptera frugiperda 21* (*Sf21*) insect cells. Full-length Btk (Met1-Ser659) was expressed with an N-terminal His-tag (MHHHHHH) and a C-terminal Flag-tag (DYKDDDDK), and was designated His-hBtk-FL-Flag. The kinase domain construct, hBtk KD P385−S659, was expressed with an N-terminal His-tag followed by a thrombin cleavage site (MGHHHHHHGSLVPRGS). The constructs were generated by PCR amplification using a full-length cDNA and were cloned into pDEST8 (Invitrogen, Carlsbad, CA). The plasmids were transformed and clonal isolates were DNA sequence confirmed.

The His-hBtk-FL-Flag and hBtk KD P385-S659 constructs were recombined and transfected into insect cells using Invitrogen's BaculoDirect Expression kit (Invitrogen Carlsbad, CA) following the protocol recommended by the manufacturer. The P1 virus from clonal isolates expressing full-length and kinase domain Btk were amplified in a suspension culture of *Sf9* cells at a density of 5×10^5 cells/mL and a multiplicity of infection (MOI) of 0.5 pfu/cell. The amplified high titer virus (HTV) was then used to infect *Sf21* cells at a density of 2.0×10 (*6*) cells/mL using an MOI of 2.0 pfu/cell. The cells were harvested by centrifugation at 72 h post infection (HPI), resuspended in 5 mL PBS-CMF/L, flash frozen dropwise into liquid nitrogen, and then stored at −80 °C.

For full-length Btk purification, the insect cells were resuspended in lysis buffer containing 50 mM Tris−HCl pH 8.5, 200 mM NaCl, 15 mM imidazole, 5 mM β-mercaptoethanol, 5 mM B-glycerophosphate, 0.1 mM orthovanadate, 50 mM sodium fluoride, and protease complete EDTA-free

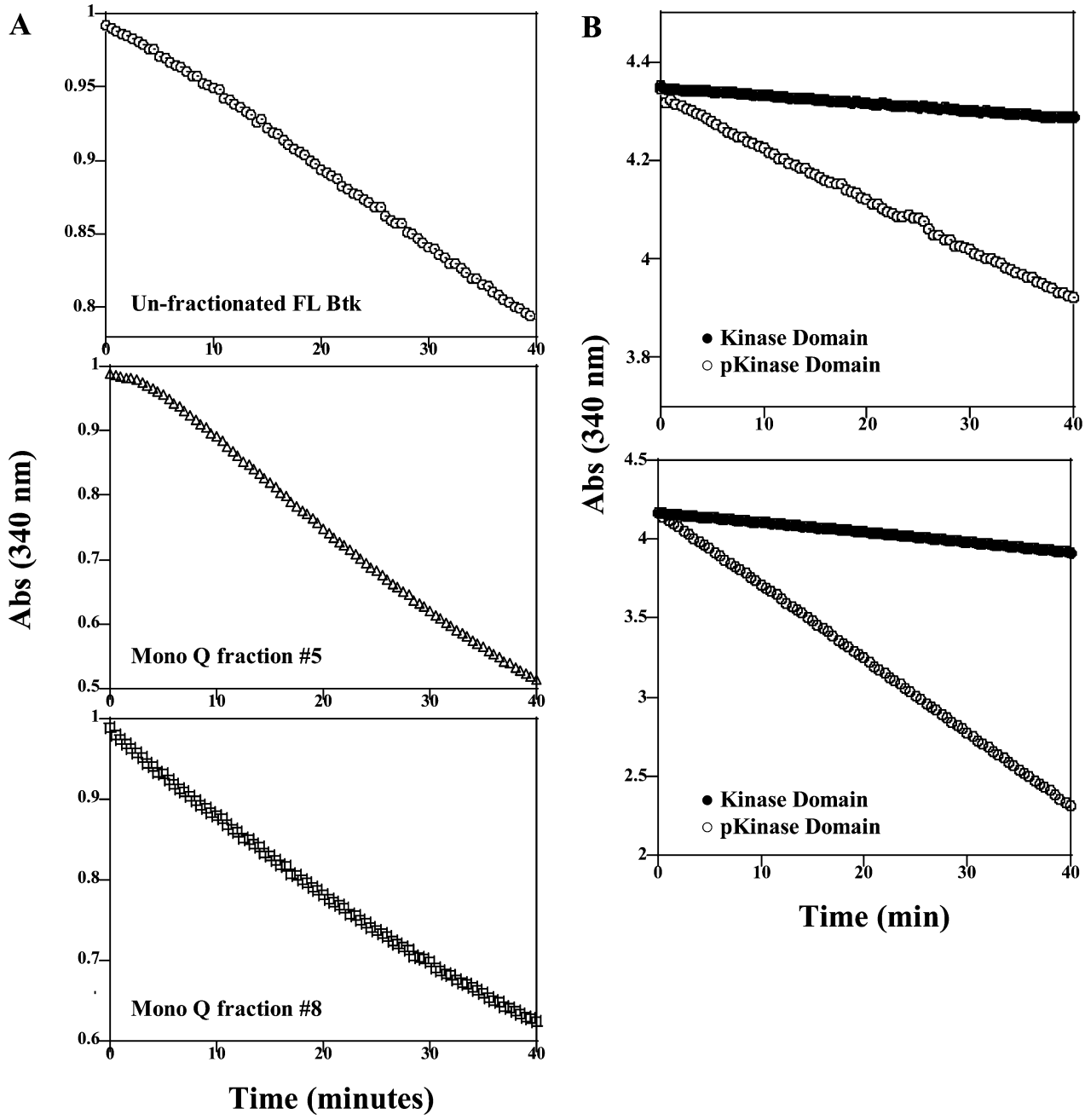

FIGURE 2: Initial activity profile of various Btk fragments. Reactions were carried out in a buffer containing 25 mM HEPES pH 7.5, 10 mM $MgSO_4$, 0.008% Triton, 1 mM ATP, and 0.2 mg/mL poly EY or 0.5 mM Y223 as the substrate. Enzyme concentrations were at 25 nM for the full-length protein and 25−100 nM for the kinase domain. Reactions were initiated by the addition of the enzyme. (A) Top: unfractionated full-length Btk. Middle: Mono Q fraction #5. Bottom: Mono Q fraction #8. The samples have an observed V_{max} of 198, 174, and 152 min^{-1}, respectively. (B) Initial rate analyses of the unphosphorylated Btk kinase domain (KD) (●) and its phosphorylated counterpart (pKD) (○). Top panel: reaction carried out in the presence of poly EY substrate. The observed V_{max} for KD is 3.0 min^{-1} and for pKD is 21 min^{-1}. Bottom panel: initial rate analyses using Y223 as the substrate. Btk KD produced an observed V_{max} of 12.4 min^{-1}, while pKD resulted in a V_{max} of 137 min^{-1}.

inhibitor cocktail (Roche). Cells were stirred at 4 °C for 15 min and then centrifuged at 12000*g* for 30 min. The supernatant was loaded onto a HisTrap FF column (GE Healthcare) pre-equilibrated with buffer A1 (50 mM Tris−HCl pH 8.0, 500 mM NaCl, 25 mM imidazole, 5 mM β-mercaptoethanol). The column was washed with buffer A1 and then with buffer A2 (50 mM Tris−HCl pH 8.5, 50 mM NaCl, 35 mM imidazole, 5 mM β-mercaptoethanol) and eluted with buffer B containing 50 mM Tris−HCl pH 8.0, 50 mM NaCl, 500 mM imidazole, and 5 mM β-mercaptoethanol. Btk-containing fractions were pooled and diluted 3-fold with buffer C (20 mM Tris−HCl, pH 8.0, 2 mM DTT), before loading onto a POROS HQ 20 column (4.6 × 100 mm) (Applied Biosystems) pre-equilibrated with buffer C. The column was developed with a linear NaCl gradient up to 1.0 M in buffer C. Btk fractions were combined and applied onto a 5 mL hydroxyapatite column (BioRad Laboratories, Hercules, CA) pre-equilibrated with buffer D (5 mM sodium phosphate, pH 8.0, 5 mM DTT) and eluted with a sodium phosphate gradient up to 500 mM in buffer D. Btk-containing fractions were concentrated and further purified on a Superdex 16/60 gel permeation column (GE Healthcare) using 20 mM Tris−HCl, pH 7.5, 200 mM NaCl, and 2 mM TCEP as the running buffer (buffer E). All purification steps were done

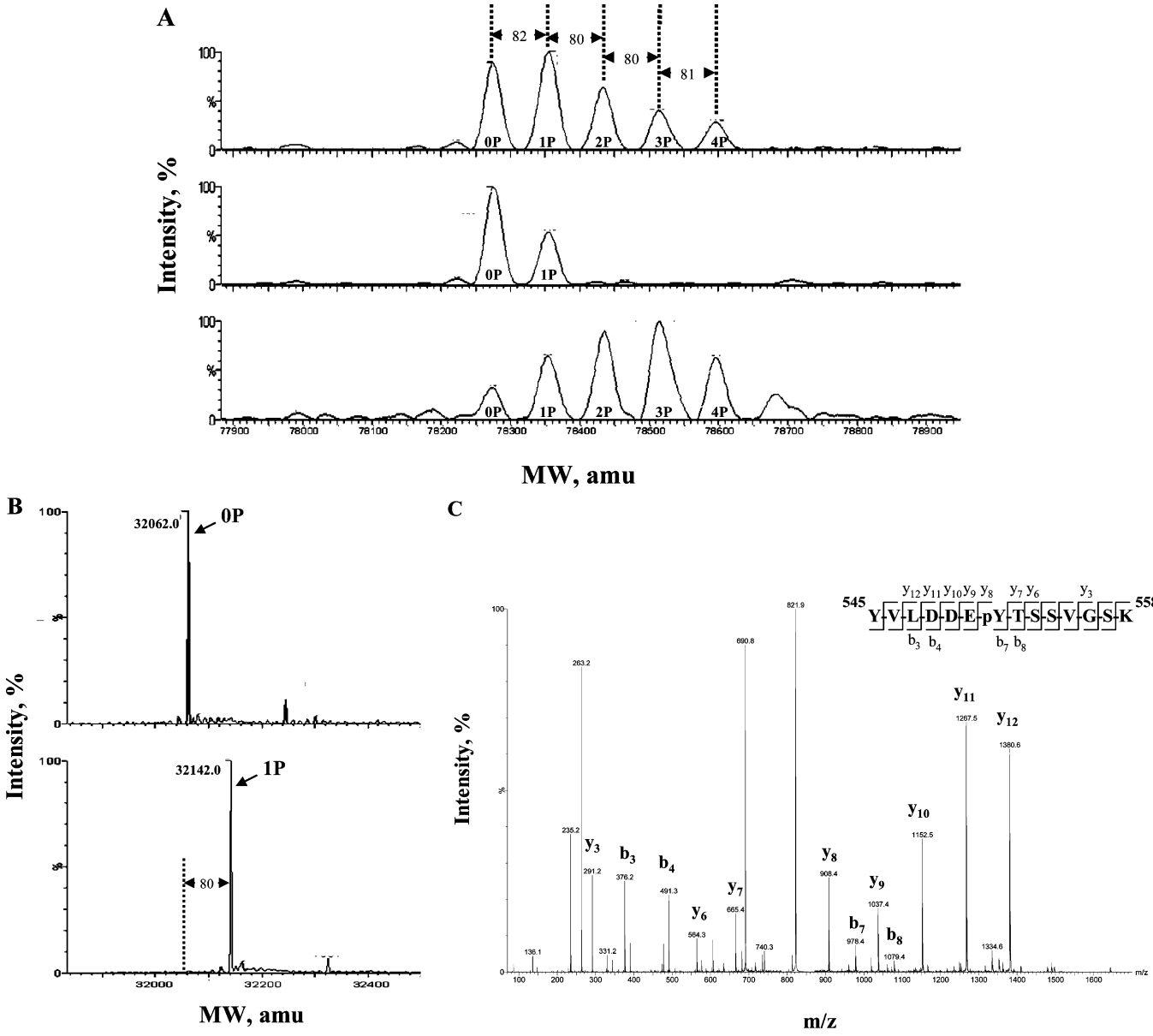

FIGURE 3: LC−MS characterization of Btk phosphorylation status. (A) Top: unfractionated full-length Btk. Middle: Mono Q fraction #5. Bottom: Mono Q fraction #8. Both Mono Q fractions are of full-length enzymes. The MS species 0P through 4P have the corresponding molecular weight of 78 274, 78 356, 78 436, 78 516, and 78 597 Da, respectively. The lowest MS species of 78 274 Da represents the unphosphorylated full-length Btk (molecular weight of 78 230) with an N-terminal acetylation. The protein was found to be N-terminal blocked. The mass difference of ca. 80 Da among the higher molecular weight species correlates with the addition of a single phosphate group. Attempts were made to map these phosphorylation sites using trypsin digestion and microLC isolation of the resulting peptides. ESI-MS analysis identified Y^{551} as the prevalent phosphorylation site. The Y223-containing peptides were not identified from the tryptic mixture; therefore, Y^{223} phosphorylation could not be verified. (B) Top: unphosphorylated Btk kinase domain. Bottom: Lyn activated and purified Btk kinase domain. The lowest molecular weight species of 32 062 Da matches well with the calculated molecular weight (32 061 Da). The MS difference between the two samples accounts for the addition of a single phosphate group. (C): MS/MS of peptide YVLDDEYTSSVGSK (residues 545−558). The Mono Q purified, phosphorylated Btk kinase domain (same sample as in Figure 3B bottom panel) was digested with trypsin as described in the Experimental Procedures section. The resulting peptides were analyzed using reverse-phase microLC. The phosphorylated peptide YVLDDEYTSSVGSK was identified, and MS/MS of the product ion spectrum indicated that Y^{551} was the phosphorylation site. For reasons of clarity, only selected species are labeled.

at 4 °C except the hydroxyapatite step, which was carried out at room temperature with cooled buffers.

For the Btk kinase domain purification, the cells were lysed in 50 mM Tris−HCl, pH 8.0, 200 mM NaCl, 5 mM imidazole, 5 mM β-mercaptoethanol, and protease Complete EDTA-free inhibitor cocktail. The cell lysate was clarified by centrifugation at 4 °C, and the supernatant was loaded onto a HisTrap FF column. Affinity purification was carried out following the same procedure as full-length Btk. Fractions containing Btk kinase domain were pooled and 10-fold diluted with buffer C and loaded onto a tandem Poros HS/HQ column. The HS column was taken offline, and Btk kinase domain was eluted from the HQ column via a linear NaCl gradient up to 1.0 M in buffer C. Btk KD fractions were pooled and digested with thrombin protease (GE Healthcare, Piscataway, NJ) at 4 °C overnight at a ratio of 1 unit/50 μg Btk protein. Further purification was achieved by a TSK-G3000 gel permeation column (Tosoh Biosciences) using buffer E as the mobile phase. Both Btk FL and KD proteins were shown to be >95% pure based on their profiles

on the analytical gel filtration column and by mass spectrometry analysis.

In Vitro Phosphorylation and Isolation of Phosphorylated Btk Kinase Domain. Active Lyn and Syk were obtained from Upstate Biotech (Cat. #14-510 and 14-314, Millipore, MA). Scale-up phosphorylation was carried out in Tris−HCl, pH 7.5, 0.1 mM EGTA, 0.1 mM orthovanadate, 0.1% B-mercaptoethanol, 8 mM ATP, and 10 mM $MnCl_2$, using a Btk to Lyn molar ratio of 500:1. The reaction mixture was incubated for 3 h at room temperature, and Btk phosphorylation was monitored by Western blot analysis using antiphosphotyrosine 551 antibody (Cat. #558034, BD Biosciences Pharmingen, San Diego, CA). The resulting phosphorylated Btk kinase domain was separated from the unphosphorylated material by a Mono Q HR5/5 column (GE Healthcare, Piscataway, NJ) using a linear NaCl gradient up to 0.5 M over 25 column volumes.

MicroLC ESI-MS Characterization of Btk Protein Phosphorylation States and Phosphorylation Site Mapping. The phosphorylation states of various Btk proteins were determined by microLC ESI-MS. The samples were injected onto an Agilent 1100 HPLC system equipped with a reverse-phase C4 Symmetry 300 column (1 × 150 mm, 3 μm particle size, Waters Corporation, Milford, MA) with a set flow rate of 50 μL/min. The HPLC gradient increased from 10% to 90% B over a period of 60 min, where A is water with 0.1% formic acid and B is acetonitrile with 0.1% formic acid. The ESI-MS data were acquired using a Waters-Micromass LCT mass spectrometer. The cone voltage was set to 35 V, and the HPLC eluate for the first 10 min, containing salts and buffer, was diverted to waste. The acquired protein data were smoothed, background subtracted, centroided, and transformed for molecular weight determination using the Micromass component analysis software. The observed components were confirmed using the Micromass maximum entropy algorithm. The resulting maximum entropy spectral peaks were integrated for calculation of the phosphate distribution in the protein.

For identification of phosphorylation sites by mass spectrometry, Btk proteins were digested with sequencing grade trypsin (Sigma) at 1:10 trypsin:Btk (w/w) ratio at room temperature overnight. The reaction mixture was checked by SDS-PAGE for completion. MicroLC ESI-MS/MS was used to analyze the peptides. The samples were injected onto an Agilent 1100 HPLC system equipped with a reverse-phase C18 Symmetry 300 column (1 × 150 mm, 3 μm particle size, Waters Corporation, Milford, MA) with a set flow rate of 65 μL/min. The peptides were eluted with a linear gradient of 10% to 90% B over a period of 90 min, where A is water with 0.1% formic acid and B is acetonitrile with 0.1% formic acid. The ESI-MS/MS data were acquired using a Waters-Micromass q-Tof Micro mass spectrometer with both negative and positive ionization modes with high and low collision energies. In the negative mode, the low energy mode produces the normal spectrum while the high energy produces characteristic *m/z* 79 (1−) ions indicative of phosphorylation. In the positive ionization mode, low CE mode produces the normal spectrum while high CE may produce parent ions with losses of phosphate groups.

Kinase Kinetics. Btk activity was characterized in base buffer of 25 mM HEPES (pH 7.5), 10 mM $MgCl_2$, 25 mM NaCl, 10 mM KCl, 0.008% triton X-100, and 2 mM DTT. This base buffer was used in all assays. The kinetics was followed by linking the turnover of ATP to the turnover of NADH to NAD. NADH depletion was followed spectrophotometrically at 340 nm. The continuous assay solution contained 20 units of pyruvate kinase, 30 units of lactate dehydrogenase, 0.25 mM NADH, and 2 mM PEP. A typical assay contained 25 nM FL Btk, 20 nM Btk pKD, or 100 nM Btk KD. Reactions were allowed to equilibrate for several minutes before initiating the reaction with peptide or ATP. All reactions were done in duplicate. The kinetic measurements were carried out in a 384-well plate at 25 °C, on a Molecular Devices spectrophotometer.

HPLC Assay. The enzymatic assays in which total Mg^{2+} was varied were analyzed on an Agilent 1100 HPLC using a Phenomenex Auga 5 μm C18 125 Å 50 mm × 4.60 mm column (00B-4299-E0). Phosphorylated peptide was separated from nonphosphorylated peptide using a gradient of 0% to 100% 20 mM sodium phosphate buffer pH 8.8/acetonitrile (50/50). Elution was monitored with UV detection at 214 nm, and substrate and product peak areas were obtained using the HP Chemstation software provided with the instrument.

Data Analysis. The steady-state kinetic parameters were determined by fitting data to eq 1:

$$v = V_{max}[S]/K_m + [S] \quad (1)$$

V_{max} is the maximal velocity, and K_m is the Michaelis constant.

For dead-end inhibition, data were fit to eq 2 for competitive inhibition, eq 3 for noncompetitive inhibition, and eq 4 for uncompetitive inhibition.

$$v = V_{max}[S]/K_m(1 + [I]/K_i) + [S] \quad (2)$$

$$v = V_{max}[S]/K_m(1 + [I]/K_i) + [S](1 + [I]/K_i) \quad (3)$$

$$v = V_{max}[S]/K_m + [S](1 + [I]/K_i) \quad (4)$$

K_i is the inhibition constant for substrate inhibition.

For initial velocity, data were fit to eq 5

$$v = V_{max}[A][B]/\alpha K_a K_b + K_a[B] + K_b[A] + [A][B] \quad (5)$$

K_a and K_b are the Michaelis constants for A and B, and α is the ratio of the dissociation constant of the binary EA complex and the Michaelis constant K_a. The concentration of free Mg^{2+} was determined using the following equation:

$$[Mg^{2+}]_{free} = [Mg^{2+}]_{total} - [Mg\text{-}ATP]$$

for the HPLC assay, and

$$[Mg^{2+}]_{free} = [Mg^{2+}]_{total} - [Mg\text{-}ATP] - [Mg\text{-}PEP] - [Mg\text{-}NADH]$$

for the pyruvate kinase/lactate dehydrogenase coupled assay using the dissociation constants of 0.014 mM for [Mg-ATP], 5 mM for [Mg-PEP], and 19.5 mM for Mg-NADH (*26*).

The data were analyzed using Sigma Plot 2000 Enzyme Kinetics Module from SPSS Science (Richmond, CA).

RESULTS

In an effort to understand the detailed molecular mechanisms governing Btk activation and activity, we expressed both full-length Btk and the Btk kinase domain in Baculovirus infected *Spodoptera frugiperda 21* (*Sf21*) insect cells.

Both proteins were purified to homogeneity as described in the Experimental Procedures section. Coomassie Blue staining and MS analysis showed that both enzymes are >95% pure (Figure 1B).

Btk Activity Evaluation. Enzyme kinetic analysis for both full-length Btk and its kinase domain was carried out using a coupled assay linking the ATP turnover to the turnover of NADH to NAD as described under the Experimental Methods section. Product formation was monitored as a function of time. Using a peptide substrate poly Glu-Tyr (poly EY), we observed a lag phase of ~40−60 s in Btk product formation for the full-length enzyme (Figure 2A top panel), most likely the result of autophosphorylation on Y^{551} (*25*). ESI-MS analysis indicated that the full-length enzyme was heterogeneously phosphorylated, ranging from 0 to 4 phosphate groups, with 0 and 1 phosphate as the most abundant species (Figure 3A, top panel). Preliminary microLC−MS/MS analysis of this sample identified Y^{551} as the most prominent phosphorylation site. A Mono Q anion exchange column was used to partially separate the different phosphorylated forms. As shown by ESI-MS analysis, a Mono Q elution fraction (#5) had mostly 0 phosphate and some 1 phosphate, whereas fraction #8 was highly phosphorylated with only minor amount of unphosphorylated species (Figure 3A, middle and bottom panel). When these two fractions were tested in the coupled enzymatic assay, the lag phase was more pronounced in the less phosphorylated sample (Figure 2A middle panel, ~120 s) but largely eliminated in the highly phosphorylated fraction #8 (Figure 2A bottom panel), suggesting that a higher degree of phosphorylation contributed directly to the rate of kinase activation. Regardless of the phosphorylation status, after a 10 min incubation all samples reached a similar V_{max} of 198, 174, and 152 min^{-1}, respectively (see Figure 2 legend). Next, we tested the Btk kinase domain construct using the same assay format. As shown in Figure 2B (top panel), the Btk kinase domain had very low enzymatic activity when the same poly EY peptide substrate was used. The V_{max} for the reaction was merely 3.0 min^{-1}, 60 fold slower than that for the full-length enzyme. Furthermore, no lag phase was observed for the kinase domain, suggesting the lack of autophosphorylation for this construct. Further ESI-MS analysis indicated that the Btk kinase domain, when overexpressed in the insect cells, was unphosphorylated (Figure 3B, top panel). This result differs significantly from the Src family kinases where the kinase domains can be expressed as phosphorylated, highly active enzymes (*27, 28*). Preincubation of Btk kinase domain with Mg^{2+}/ATP did not significantly improve its kinase activity (data not shown).

Generation of in Vitro Phosphorylated Btk Kinase Domain. To determine whether the lack of phosphorylation for the Btk kinase domain is the primary reason for its low enzymatic activity, we decided to explore the possibility of phosphorylating the Btk kinase domain in vitro using its upstream kinases Lyn and Syk, as well as FL-Btk. The use of FL-Btk is based on previous reports that Btk is capable of autophosphorylation on Y^{551} (*25, 29*). Upon incubation with various enzymes, Btk kinase domain phosphorylation was probed using Western blot analysis with a phosphor-Tyrosine 551-specific antibody. Samples treated with either Lyn or Syk produced a very strong signal on the Western blot in a dose-dependent manner (Figure 4, lane 4−7),

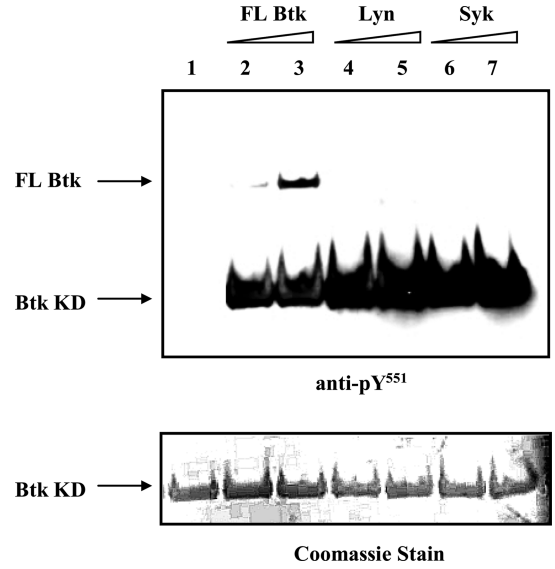

FIGURE 4: In vitro phosphorylation studies of Btk kinase domain. Top: Western blot analysis of kinase domain phosphorylation catalyzed by full-length Btk, Lyn, and Syk. The reaction mixture contained 50 mM Tris−HCl, 0.1 mM EGTA, 0.1 mM sodium orthovanadate, 0.1% β-mercaptoethanol, and either 8 mM ATP/20 mM $MgSO_4$ (shown) or 8 mM ATP/10 mM $MnCl_2$. The protein concentration for the reaction was 15 μM, with a molar ratio of protein/activating enzyme of 500:1 or 100:1. The reaction was incubated for up to 3 h at 25 °C. Longer incubation did not result in a further increase in signal. A total of 10 μg of protein per sample was loaded onto a 10−20% SDS-PAGE, transferred onto a PVDF membrane, and probed with a pY^{551} specific antibody. Bottom: Coomassie staining of the PVDF membrane.

whereas the untreated control sample was unreactive (lane 1). Samples incubated with FL-Btk also generated a positive signal but not as strong as the ones treated with Lyn or Syk (lane 2 + 3). This finding confirms that, at least in vitro, FL-Btk is capable of autophosphorylation on Y^{551}. A second blot probed with a phosphor-tyrosine specific antibody 4G10 is included in the Supporting Information for comparison (Figure S1). Next, we evaluated the optimal ratio of the Btk kinase domain to the activating enzyme, Lyn, and the effects of Mg^{2+} to Mn^{2+} in various buffers. It was found that Mn^{2+} in Tris−HCl buffer with a Btk kinase domain/Lyn molar ratio of 500:1 produced the optimal condition for activation (data not shown). A scale-up phosphorylation was performed and a Mono Q high-resolution anion exchange column was used to separate the phosphorylated Btk kinase domain from the unphoshorylated species. Subsequent evaluation of this material using ESI-MS indicated that the protein was uniformly monophosphorylated (Figure 3B, bottom panel). A complete tryptic digestion was performed on this sample. The resulting peptide mixture was subjected to reverse-phase microLC, and further analysis using ESI-MSMS mapped the phosphorylation site unambiguously to the activation loop Y^{551} (Figure 3C). To determine whether phosphorylation of Y^{551} altered the kinase domain activity, we carried out the coupled assay under the identical condition used for the unphosphorylated kinase domain. Figure 2B (top panel) showed that the activation loop phosphorylation indeed increased the kinase domain enzymatic activity, reaching a V_{max} of 21.0 min^{-1}, 7-fold higher than that of the kinase domain. As in the case of unphosphorylated kinase domain, no lag phase was observed during the reaction, suggesting no further Y^{551} autophosphorylation. To evaluate whether

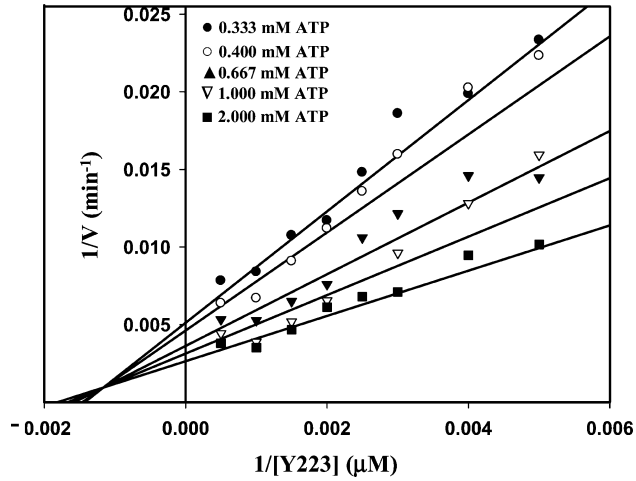

FIGURE 5: Initial velocity kinetics of the phosphorylated Btk kinase domain. The initial velocity of the reaction was determined as a function of Y223 peptide substrate concentration at varied ATP concentrations (●, 0.333 mM ATP; ○, 0.4 mM ATP; ▲, 0.667 mM ATP; ▽, 1 mM ATP; ■, 2 mM ATP). The double-reciprocal Lineweaver−Burk plot produced a $K_{a(ATP)}$ of 823 ± 403 μM and a $K_{b(Y223)}$ of 860 ± 460 μM, with an α value of 0.56.

Table 1: Peptide Sequences Used in Current Study

peptide name	sequence	function	pI
poly EY (4:1)	MW 20 000−50 000	substrate	NA
Y223 (Btk peptide)	KKVVALYDYMPMN-CONH2	substrate	8.43
gastrin	GPWLEEEEEAYGWM-CONH2	substrate	3.51

this increase in kinase activity was substrate dependent, a Y223 peptide derived from the Btk Y^{223} autophosphorylation site was used in the coupled assay. As shown in Figure 2B bottom panel, Y^{551} phosphorylation once again led to a significant increase in kinase domain activity resulting a V_{max} of 137 min^{-1} compared to a V_{max} of 12.4 min^{-1} for the unphosphorylated kinase protein. No lag phase was seen with either form of the kinase domain. Further, the Y223 peptide seemed to be a better substrate than poly EY for the kinase domain fragment on the basis of the observed higher turnover rate.

Steady-State Kinetic Analysis Indicated That upon Y^{551} Phosphorylation, Btk Kinase Domain Has Comparable Activity as the Full-Length Enzyme. Having generated a homogeneously phosphorylated Btk kinase domain allowed us to further characterize the effect of Y^{551} phosphorylation on Btk catalytic activity. Table 1 lists the peptide substrates used for the steady-state kinetic parameter determination. In addition to the poly EY and Y223 peptides used in the initial rate analysis, a third peptide substrate derived from amino acid 77−92 of human gastrin protein was also included for comparison. Steady-state kinetic constants were determined by varying either ATP or peptide substrate concentration while holding the other constant. As shown in Table 2a, activation loop phosphorylation appears to have significantly shifted the Btk kinase domain to a more active conformation. Regardless of the peptide substrate used, Y^{551} phosphorylation resulted in at least a 10-fold increase in the overall kinase activity (k_{cat}/K_m) when compared to the kinase activity of its unphosphorylated counterpart (columns 4, 7, and 10). With the exception of poly EY peptide substrate, the resulting phosphorylated kinase domain has an equivalent or better enzymatic activity than FL-Btk. This increase in k_{cat}/K_m is largely from the significant increase in the reaction k_{cat} upon Y^{551} phosphorylation (500 min^{-1} vs 99 min^{-1} for Y223, 139 min^{-1} vs 7 min^{-1} for gastrin, and 59 min^{-1} vs 2 min^{-1} for poly EY). For the two sequence specific peptide substrates Y223 and gastrin, the K_m values for peptide binding varied within 2−3 fold for all three constructs (Table 2a, columns 2 and 5). The nonspecific poly EY peptide was shown to be a particularly weak substrate for the unphosphorylated Btk kinase domain. We were not able to get an accurate K_m measurement for this peptide substrate. Upon Y^{551} phosphorylation, the kinase domain is able to bind the poly EY peptide more efficiently, producing a K_m of 1.1 mg/mL. FL-Btk enzyme has the highest binding affinity for this peptide substrate. As for the second substrate, ATP, once again we observed a similar trend: both kinase domain proteins have a similar apparent K_m for the substrate that is within 2-fold of the full-length enzyme. The reaction k_{cat} for the unphosphorylated kinase domain is significantly slower which has led to a 5-fold reduction in the catalytic efficiency (k_{cat}/K_m) when compared to the phosphorylated kinase domain, which has a similar activity as the full-length enzyme (Table 2b, column 2). In all three constructs, the absence of peptide substrate has resulted in a 60−70-fold decrease in the rate of ATP hydrolysis (k_{cat}^a). The K_m values for ATP (no peptide, K_m^a) were slightly elevated for FL-Btk and the phosphorylated kinase domain and significantly increased (6-fold) for the unphosphorylated kinase domain construct. The difference in K_m values for ATP in the presence and absence of peptide substrate mostly reflects a potential synergistic effect between ATP and peptide binding sites.

Inhibitor Binding Studies. Next, we compared the Btk kinetic mechanism with or without the context of its noncatalytic domains. Using the Y223 substrate peptide, we were able to perform an initial velocity analysis for FL-Btk and determined that FL-Btk followed a sequential kinetic mechanism (data not shown). This result is consistent with a recent study showing that FL-Btk employs a ternary complex mechanism, in which the binding of peptide substrate S1 and ATP is either random or ordered with ATP binding first (*25*). Furthermore, we observed on the double-reciprocal plots an α factor of 0.71. The α value is a measure proportional to the extent of interactions between substrate sites (*30*). A value of <1 implies a positive effect of one substrate binding (ATP or peptide) upon binding of the other. This result is different from the one obtained by Dinh et al. (α value of 3.1) (*25*). Several factors can potentially contribute to this discrepancy, such as assay format and peptide substrate. Because of the lag pase in Btk activation, the enzyme used in our study was preincubated with Mg^{2+}/ATP. This step was necessary to eliminate any differences in the rate of activation due to a varying amount of ATP in the reaction. Moreover, the substrate used by Dinh et al. (Aca-AAAEEIYGEI-NH_2) (*25*), is significantly different from the Y223 peptide used in this study. In fact, when we repeated the same experiment using the poly EY substrate, we obtained an α value of 2.1, suggesting that the interactions between substrate sites is peptide-sequence dependent.

To evaluate whether isolated, phosphorylated kinase domain followed a similar kinetic mechanism as the full-length enzyme, we carried out initial reaction velocity determination at varying ATP and Y223 peptide concentra-

Table 2: Steady-State Kinetic Parameters

(a) For Peptide Substrates

protein name	$_{app}K_m$ (Y223) (mM)	k_{cat} (min^{-1})	k_{cat}/K_m (M^{-1} s^{-1})	$_{app}K_m$ (gastrin) (mM)	k_{cat} (min^{-1})	k_{cat}/K_m (M^{-1} s^{-1})	$_{app}K_m$ (poly EY) (mg/mL)	k_{cat}(min^{-1})	k_{cat}/K_m (mg^{-1} s^{-1})
FL Btk	1.3 ± 0.2	215 ± 27	2756	2.1 ± 0.3	142 ± 14	1127	0.122 ± 0.035	106 ± 6	14.5
KD	3.4 ± 0.5	99 ± 11	485	1.7 ± 0.4	7 ± 1	67	ND	~2[a]	
pKD	1.6 ± 0.2	500 ± 36	5208	1.3 ± 0.4	139 ± 22	1782	1.1 ± 0.1	59 ± 2	0.894

(b) For ATP

protein name	$_{app}K_m$[b] (ATP) (μM)	k_{cat}[b] (min^{-1})	k_{cat}/K_m (M^{-1} s^{-1})	$_{app}K_m$[c] (ATP) (μM)	k_{cat}[c] (min^{-1})	k_{cat}/K_m (M^{-1} s^{-1})
FL Btk	232 ± 28	215 ± 27	15445	650 ± 50	3.2 ± 0.1	82
KD	425 ± 35	99 ± 11	3882	2500 ± 700	1.6 ± 0.2	11
pKD	440 ± 35	500 ± 36	18939	640 ± 40	6.6 ± 0.2	172

[a] Velocity measurement at the highest concentration of poly EY (2 mg/mL). [b] With 0.5 mM Y223 peptide. [c] In the absence of peptide substrate.

Table 3: Inhibition Patterns

(a) For the Phosphorylated Btk Kinase Domain

inhibitor	substrate	K_i (mM)	mode	inhibitor type
AMPPNP	ATP	0.630 ± 0.041	C	deadend
AMPPNP	Y223	3.1 ± 0.4	NC	deadend
5-IT	ATP	0.338 ± 0.057	C	deadend
5-IT	Y223	0.216 ± 0.079	NC	deadend

(b) For Full-Length Btk

inhibitor	substrate	K_i (mM)	mode	inhibitor type
AMPPNP	ATP	0.290 ± 0.020	C	deadend
AMPPNP	Y223	2.2 ± 0.1	NC	deadend
5-IT	ATP	0.109 ± 0.008	C	deadend
5-IT	Y223	0.204 ± 0.048	NC	deadend

tions. The resulting data produced an intersecting pattern in the double-reciprocal Lineweaver−Burk plot, characteristic of a sequential or ternary complex mechanism (Figure 5). The plot produced an α factor of 0.56, similar to that observed for the full-length enzyme. Together these results indicated that the enzymatic mechanism of human Btk is not affected by the removal of its noncatalytic domains. We next compared the inhibition kinetics of these two constructs using the nonhydrolyzable ATP analogue, AMP-PNP, and 5-iodotubericidin (5-IT), an inhibitor of adenosine kinases and protein kinases including MAP kinase ERK2 (*31*). AMP-PNP was shown to be a competitive inhibitor of ATP for both constructs with a K_i value of 0.63 mM for the phosphorylated kinase domain and 0.29 mM for the FL enzyme (Table 3). 5-IT, like AMP-PNP, was found to be a competitive inhibitor of ATP with a generally 2-fold lower K_i value. Both inhibitors were shown to be noncompetitive of Y223 peptide with K_i values in the millimolar range for AMP-PNP and ~200 μM range for 5-IT (Table 3). None of the inhibitor peptides with tyrosine to phenylalanine substitutions showed any inhibition; therefore, substrate analog inhibition could not be evaluated in this analysis. Taken together, our analysis demonstrated that the phosphorylated Btk kinase domain followed the same kinetic mechanism as the FL enzyme with a very similar substrate inhibition pattern.

Btk Requires a Second Magnesium Ion for Activity. With the exception of poly EY substrate, our analysis so far showed that activation loop Y^{551} phosphorylation had very little effect on the K_m's for substrate binding. However, upon Y^{551} phosphorylation, there was a significant increase in the reaction k_{cat} (Table 2) for all three peptide substrates and

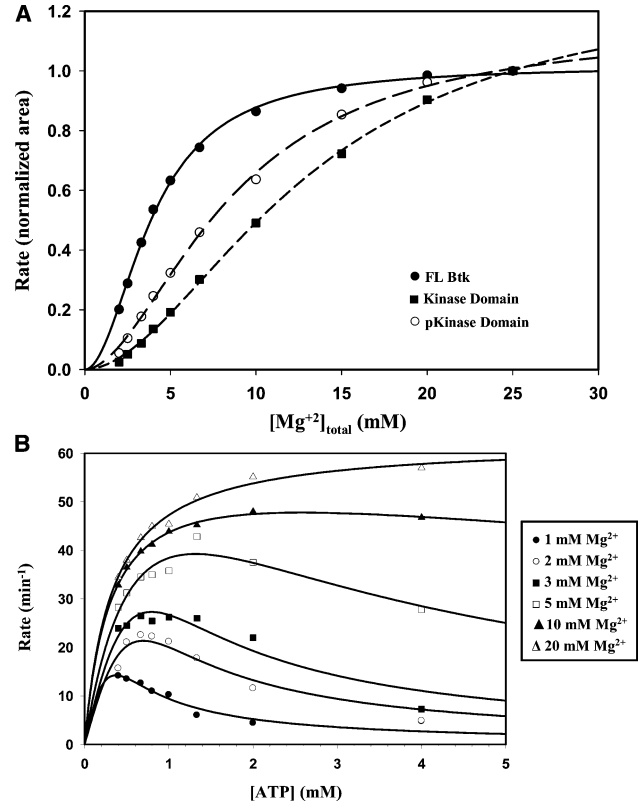

FIGURE 6: Metal dependence of Btk activity. (A) Initial velocities of Btk constructs as a function of total Mg^{2+} concentrations. The reaction was analyzed by following the formation of phosphorylated-Y223 peptide on an HPLC equipped with a C18 reverse-phase column as described in the Experimental Procedure section. All samples contained 2 mM ATP and 0.5 mM Y223 peptide (●, full-length Btk; ○, phosphorylated Btk domain; ■, unphosphorylated kinase domain). (B) ATP velocity profiles at different concentrations of total Mg^{2+} (●, 1 mM; ○, 2 mM; ■, 3 mM; □, 5 mM; ▲, 10 mM; Δ, 20 mM). The reaction was carried out using Y223 peptide, and the pyruvate kinase/lactate dehydrogenase-coupled assay was monitored by a Molecular Devices spectrometer (Experimental Section).

ATP. Since the phosphoryl-transfer step of kinases involves divalent metal ions such as magnesium, we decided to examine in more detail the effect of divalent metal ions on Btk catalysis. Once again using the coupled assay, the formation of phosphorylated peptide substrate was monitored as a function of total magnesium concentration ($[Mg^{2+}]_{total}$). The reaction was carried out in the presence of 2 mM ATP. As shown in Figure 6A, FL-Btk activity was the lowest at a $[Mg^{2+}]$/ATP ratio of 1:1 (2 mM $MgCl_2$ and 2 mM ATP).

Table 4: Kinetic Parameters of Divalent Metal Binding of Btk Enzymes

protein name	$_{app}K_{m(Mg)}$ (mM)
FL Btk	1.9 ± 0.2
KD	$32 + 2$
pKD	10 ± 1

As the magnesium concentration increased, we saw a gradual increase in kinase activity. Maximum activity was reached at 20 mM [Mg^{2+}], indicating that the additional, free [Mg^{2+}] was necessary for Btk activity. The Btk kinase domain, regardless of Y^{551} phosphorylation, exhibited a behavior similar to that of the FL enzyme, with minimal phosphorpeptide product seen at a [Mg^{2+}]/ATP ratio of 1:1 (Figure 6A, open circle and solid square for the phosphorylated and unphosphorylated kinase domain, respectively). Both kinase domains can be further activated with increasing magnesium concentration. The apparent binding affinities of the second, free magnesium (M2) can be calculated from this plot (Table 4). FL-Btk has the lowest $_{app}K_{m[Mg^{2+}\ free]}$ of 1.9 mM, whereas the phosphorylated kinase domain has an $_{app}K_{m[Mg^{2+}\ free]}$ of 10 mM. The unphosphorylated kinase domain binds only weakly to free magnesium with an $_{app}K_{m[Mg^{2+}\ free]}$ of 32 mM. These results imply that the M2 binding contributes, at least in part, to the low enzymatic activity of the Btk kinase domain. A likely scenario might be that the residues in the M2-binding site in the Btk kinase domain are misaligned. Activation loop phosphorylation helps to modulate the catalytic potential in the kinase domain by repositioning the residues involved in M2 binding.

In order to distinguish whether the second magnesium ion is an essential activator, we further evaluated ATP concentration at different fixed total magnesium concentrations using the full-length enzyme (Figure 6B). The rate of reaction increased significantly at higher magnesium concentrations, consistent with our earlier observation. At lower [Mg^{2+}] concentrations, however, we observed a peak in the velocity profile that is most evident with the lowest magnesium concentration. This behavior correlates with the notion that when the concentration of ATP approaches the concentration of magnesium ion, most of the free magnesium is sequestered as an Mg−ATP complex. The result is a significantly decreased M2 concentration and a minimal reaction velocity likely due to enzyme inactivation, suggesting that the second metal ion is an essential activator for Btk activity.

In addition to evaluating divalent metal ion on Btk activity, we further investigated the effects of ionic strength on Btk catalysis. In this study, we varied the ATP concentration while holding the concentration of Y223 peptide constant and monitored the enzyme turnover rate k_{cat} (Figure S2, Supporting Information). Interestingly, as the concentration of NaCl is increased (up to 1 M), we observed a decrease in the turnover rate for FL-Btk. A decrease was also observed for the phosphorylated kinase domain with a smaller magnitude. The unphosphorylated version of the protein, on the other hand, behaved very differently. As NaCl concentration increased, we saw a significant increase in the reaction k_{cat}. This difference between the two kinase domains further supports our earlier results suggesting a potential conformational change in Btk kinase domain upon activation loop phosphorylation.

DISCUSSION

Because of our interest in developing therapeutic antagonists of Btk, we directed our studies to understand the mechanisms that govern Btk activation and regulation. Previous studies followed Btk kinase activity using either a cell-based approach (*12*−*14*) or purified but heterogeneously phosphorylated Btk enzyme (*25, 32*). There is significant evidence suggesting that the Tec family kinases, such as Btk and Itk, are regulated differently from the Src family kinases, despite their similarity in linear domain arrangement (*32, 33*).

In the current study, we used high-resolution ion-exchange chromatography to separate different phosphorylated forms of FL-Btk generated from insect cells. We demonstrated that upon a 10 min incubation with Mg^{2+}/ATP, all phosphorylated forms had a similar V_{max}. However, the unphosphorylated species required an autoactivation step as reflected by a lag phase in the activity profile. This observation is consistent with the study by Dinh et al. (*25*) that showed preincubation of FL-Btk with Mg^{2+}/ATP eliminated the activity lag phase and also coincided with an increase in activation loop Y^{551} phosphorylation. When expressed alone, the Btk kinase domain was found to be unphosphorylated and inactive (this study and studies by Lowry et al. (*32*) and Mao et al. (*20*)); however, when the prototypical Src family kinase domain was expressed and purified from insect cells, it was shown to be phosphorylated and also retained full activity (*34, 35*). Interestingly, by phosphorylating activation loop Y^{551} of the Btk kinase domain with the Src family kinase Lyn, we generated enzyme comparable in activity to FL-Btk. This observation conflicts with a previous study of another closely related Tec family member, Itk (*36*). Phosphorylated Itk kinase domain had a 26-fold lower k_{cat} when compared to a TH-SH3-SH2-kinase domain construct. Activation loop Y^{512} phosphorylation seemed to have no impact on Itk kinase domain activity, and unexpectedly, the phosphorylated and unphosphorylated forms both crystallized in the inactive conformation.

Detailed kinetic studies clarified the differences between unphosphorylated and in vitro phosphorylated Btk kinase domain. We demonstrated that Y^{551} phosphorylated kinase domain had comparable K_m values for ATP and peptide substrates, and similar k_{cat} values as the full-length enzyme. The only exception is the poly EY peptide that binds significantly weaker to the phosphorylated kinase domain than FL-Btk, suggesting that other Btk domains might play a role in the recognition of this particular peptide substrate. In all cases, the overall kinase activity for the phosphorylated kinase domain was at least 10−20-fold higher than the unphosphorylated counterpart, a result mostly attributed to an up to 25-fold increase in k_{cat}, suggesting the activation loop phosphorylation had caused a conformational change to a more catalytically active enzyme. However, the substrate binding sites were less affected. This result correlates well with the Dinh et al. study (*25*) where the K_m values for substrates were similar to both the full-length Btk and the Y551F mutant, although the catalytic efficiency of the wild-type enzyme was 10-fold greater than that for the mutant protein. These observations place the Btk kinase domain into the nongated category in which the activation loop phosphorylation modulates solely the phosphoryl-transfer step but

not substrate binding (*37*). Dead-end inhibitor binding studies indicated that the kinetic mechanism of the phosphorylated Btk kinase domain is consistent with a random, sequential addition of substrates, similar to the kinetic mechanism for the full-length protein. The phosphorylated kinase domain had K_i values similar to those for the FL-Btk for substrate analogue inhibitors AMP-PNP and 5-IT.

The metal dependence study suggested that Btk requires a second metal ion for activity. There have been a number of studies on divalent metal ion dependence of protein kinases. These include the most extensively characterized protein kinase cAMP-dependent protein kinase (cAPK) (*38*), serine/threonine specific protein kinase ERK2 (*31*), and Btk closely related tyrosine kinases Csk and Src (*39*). Electron paramagnetic resonance studies and X-ray crystal structure identified two divalent metal-ion-binding sites within the active site of cAPK, one activating and the second one being partially inhibitory. ERK2 on the other hand, needs both metal ions for its activity. In the case of Csk and Src, in addition to the requirement of a divalent metal cation to complex with ATP, both enzymes require a second metal cation as an essential activator. The additional magnesium ion activates Csk and Src mainly by increasing their V_{max}. It does not affect the apparent $K_{m(ATP\text{-}Mg)}$ for Csk or Src. Our analysis indicated significantly higher reaction V_{max} values for all three Btk fragments in the presence of an additional magnesium ion. However, further detailed mechanistic studies will be necessary to determine whether the apparent $K_{m(ATP\text{-}Mg)}$ was affected as well.

Our study elucidated significant differences in the M2-binding site among the unphosphorylated Btk kinase domain, its phosphorylated counterpart, and full-length enzyme. In particular, the unphosphorylated kinase domain binds only weakly to the second metal ion when compared to the full-length enzyme, suggesting that residues near the M2-binding site might play an important role in enzyme activity. Furthermore, we evaluated the effects of ionic strength on Btk catalysis. Our results indicated that increasing NaCl concentration in reaction buffer led to an increase in enzymatic activity in the Btk kinase domain, while for both full-length and phosphorylated kinase domain, we saw a decrease in activity. This observation further underlines the difference between Btk kinase domain and full-length enzyme and suggests a significant conformational change between the two. One possible interpretation of the ionic effect is the disruption of salt bridges. For example, in the crystal structure of the inactive Btk kinase domain (*20*), Arg544 forms a salt bridge with Glu445 that stabilizes the inactive conformation. A high NaCl concentration could destabilize this salt bridge resulting in an increase in kinase domain activity. Although no active Btk kinase domain structure has been reported, it has been proposed, on the basis of the inactive structure, that a large conformational change involving the rearrangement of hydrogen bond network and repositioning of αC-helix is necessary to convert the enzyme into active conformation (*20*). Upon Y^{551} phosphorylation, Arg544 may be more engaged in interaction with the phosphate group of Y^{551}, freeing up Glu445 to form the salt bridge hydrogen bond with Lys430 in the active site (*20, 40*). This arrangement may facilitate the shifting of the αC helix into an active conformation. An increase in NaCl concentration could potentially disrupt this intricate hydrogen bond network, therefore decreasing the catalytic activity. Further mutational analysis would be necessary to help validate this hypothesis.

Having established that Y^{551} phosphorylation plays a crucial role in regulating Btk kinase domain activity, what are the roles for the noncatalytic domains of Btk? Btk, along with the rest of Tec family kinases, shares a similar SH3-SH2-Kinase domain arrangement with Src family tyrosine kinases. SH3 domains interact with proline-rich sequences, whereas SH2 domains bind to phosphotyrosine-containing peptide motifs. Both domains are small protein modules that mediate protein−protein interactions and occur in many proteins involved in intracellular signal transduction (*41*). In the crystal structure of the autoinhibited three domain Src (*42*−*44*) kinase, the C-terminal tail phospho-tyrosine binds to the SH2 domain, and the SH3 domain binds to the SH3-kinase domain linker regions thus forming a compact structure where surfaces of the SH2 and SH3 domains pack against the catalytic domain on the opposite side of the catalytic cleft. This constrained multidomain interaction effectively locks the kinase domain into an inactive conformation. Activation occurs when high affinity competing ligands bind to the SH3 and SH2 domains, as well as concomitant tyrosine phosphorylation on the kinase activation loop. Because of the high sequence homology, it is tempting to speculate that some of these closely related PTKs might share common mechanisms of regulation (*2, 45*). In fact, a structural analysis on the multidomain kinase c-Abl established that Abl and Src kinases share very similar interdomain control mechanisms. Like Src, c-Abl is also negatively regulated by intramolecular SH3 domain interactions with the linker and the kinase domain. Instead of the SH2 domain C-terminal regulatory tyrosine interaction in the Src family kinases, c-Abl uses an N-terminal myristoyl modification for the intramolecular interaction with the kinase domain as a downregulation mechanism (*46, 47*). The carboxyl-terminal Src kinase (Csk), on the other hand, has adopted a different regulatory mechanism (*48*). Csk contains the SH2-SH3-kinase linear domain arrangement but lacks the C-terminal regulatory tyrosine. As shown in the crystal structure of full-length Csk, the SH2 domain interacts with the N-terminal lobe of the kinase domain. However, the interactions between SH3 and the linker region of the SH2-kinase domains are absent in the Csk structure. Additional biochemical studies showed the uniquely oriented SH2 and SH3 domains of Csk act as positive regulators of kinase activity (*49*−*51*). The Tec family is unique among the SH3-SH2 kinase domain containing enzymes in that they all contain an N-terminal PH domain (with the exception of Txk which contains a palmitylation site at the N-terminus) (*52*). The PH domain serves to localize the Tec family kinases to the membrane upon inositol lipid phosphorylation, whereas c-Abl and Src localize to the membrane via a myristylation site on the N-termini of the enzymes. Apart from this similarity, the Tec family kinases, like Csk, lack a C-terminal regulatory tyrosine. A recent biochemical study using multiple Itk deletion mutants demonstrated that Itk, and most likely other Tec kinases, are regulated in a manner more like Csk vs the Src family kinases (*33*). Deletion or mutation of the SH3 or SH2 domain in the Src family results in an increase in kinase activity; consequently, the noncatalytic domains serve as a negative regulatory function. Our current study suggests the

Btk SH2 and SH3 domains, like Csk, play an opposite, positive regulatory role. By deleting the PH, SH3, and SH2 domains, the resulting kinase exhibits rather poor catalytic activity, and this low activity is due to the lack of phosphorylation on activation loop Y^{551}. The presence of the noncatalytic domains allows the enzyme to be more efficiently autophosphorylated and activated. Studies on the closely related Itk kinase seemed to be consistent with this view (*33*). Our Mono Q fractionated FL Btk, although mostly unphosphorylated (fraction #5), is capable of autoactivation resulting in a V_{max} comparable to that of the phosphorylated species. Moreover, preliminary analyses of three-domain (SH3-SH2-KD) and two-domain (SH2-KD) Btk constructs indicated a higher degree of phosphorylation and activity (unpublished results). Together these data support a positive regulatory role by the noncatalytic domains of Btk.

ACKNOWLEDGMENT

We thank Kevin Bean for the generation of FL Btk virus and Dr. Kathy Underwood for carrying out the initial FL Btk purification. We are grateful to Drs. Will Somers and John Douhan for valuable support and critical reading of this manuscript.

SUPPORTING INFORMATION AVAILABLE

Experimental data on in vitro phosphorylation of Btk kinase domain probed with phospho-tyrosine specific antibody 4G10 and the study of ionic strength on Btk catalysis. This material is available free of charge via the Internet at http://pubs.acs.org.

REFERENCES

1. Manning, G., Whyte, D. B., Martinez, R., Hunter, T., and Sudarsanam, S. (2002) The protein kinase complement of the human genome. *Science 298*, 1912–1934.
2. Blume-Jensen, P., and Hunter, T. (2001) Oncogenic kinase signalling. *Nature 411*, 355–365.
3. Lindvall, J. M., Blomberg, K. E. M., Valiaho, J., Vargas, L., Heinonen, J. E., Berglof, A., Mohamed, A. J., Nore, B. F., Vihinen, M., and Smith, C. I. E. (2005) Bruton's tyrosine kinase: cell biology, sequence conservation, mutation spectrum, siRNA modifications, and expression profiling. *Immunol. Rev. 203*, 200–215.
4. Tsukada, S., Saffran, D. C., Rawlings, D. J., Parolini, O., Allen, R. C., Klisak, I., Sparkes, R. S., Kubagawa, H., Mohandas, T., and Quan, S. (1993) Deficient expression of a B cell cytoplasmic tyrosine kinase in human X-linked agammaglobulinemia. *Cell 72*, 279–290.
5. Vetrie, D., Vorechovsky, I., Sideras, P., Holland, J., Davies, A., Flinter, F., Hammarstrom, L., Kinnon, C., Levinsky, R., Bobrow, M., Smith, C. I. E., and Bentley, D. R. (1993) The gene involved in X-linked agammaglobulinaemia is a member of the src family of protein-tyrosine kinases. *Nature 361*, 226–233.
6. Rawlings, D. J., Saffran, D. C., Tsukada, S., Largaespada, D. A., Grimaldi, J. C., Cohen, L., Mohr, R. N., Bazan, J. F., Howard, M., and Copeland, N. G. (1993) Mutation of unique region of Bruton's tyrosine kinase in immunodeficient XID mice. *Science 261*, 358–361.
7. Thomas, J. D., Sideras, P., Smith, C. I., Vorechovsky, I., Chapman, V., and Paul, W. E. (1993) Colocalization of X-linked agammaglobulinemia and X-linked immunodeficiency genes. *Science 261*, 355–358.
8. Vassilev, A. O., Tibbles, H. E., DuMez, D., Venkatachalam, T. K., and Uckun, F. M. (2006) Targeting JAK3 and BTK Tyrosine Kinases with Rationally-Designed Inhibitors. *Curr. Drug Targets 7*, 327–343.
9. Backesjo, C. M., Vargas, L., Superti-Furga, G., and Smith, C. I. (2002) Phosphorylation of Bruton's tyrosine kinase by c-Abl. *Biochem. Biophys. Res. Commun. 299*, 510–515. (2003) Erratum. *Biochem. Biophys. Res. Commun. 301*, 259.
10. Kurosaki, T., and Kurosaki, M. (1997) Transphosphorylation of Bruton's Tyrosine Kinase on Tyrosine 551 Is Critical for B Cell Antigen Receptor Function. *J. Biol. Chem. 272*, 15595–15598.
11. Mahajan, S., Fargnoli, J., Burkhardt, A. L., Kut, S. A., Saouaf, S. J., and Bolen, J. B. (1995) Src family protein tyrosine kinases induce autoactivation of Bruton's tyrosine kinase. *Mol. Cell. Biol. 15*, 5304–5311.
12. Park, H., Wahl, M. I., Afar, D. E., Turck, C. W., Rawlings, D. J., Tam, C., Scharenberg, A. M., Kinet, J. P., and Witte, O. N. (1996) Regulation of Btk function by a major autophosphorylation site within the SH3 domain. *Immunity 4*, 515–525.
13. Rawlings, D. J., Scharenberg, A. M., Park, H., Wahl, M. I., Lin, S., Kato, R. M., Fluckiger, A. C., Witte, O. N., and Kinet, J. P. (1996) Activation of BTK by a phosphorylation mechanism initiated by SRC family kinases. *Science 271*, 822–825.
14. Wahl, M. I., Fluckiger, A. C., Kato, R. M., Park, H., Witte, O. N., and Rawlings, D. J. (1997) Phosphorylation of two regulatory tyrosine residues in the activation of Bruton's tyrosine kinase via alternative receptors. *Proc. Natl. Acad. Sci. U.S.A. 94*, 11526–11533.
15. Kurosaki, T., and Tsukada, S. (2000) BLNK: connecting Syk and Btk to calcium signals. *Immunity 12*, 1–5.
16. Pawson, T. (2002) Regulation and targets of receptor tyrosine kinases. *Eur. J. Cancer 38*, S3–S10.
17. Shokat, K. M. (1995) Tyrosine kinases: modular signaling enzymes with tunable specificities. *Chem. Biol. 2*, 509–514.
18. Hansson, H., Mattsson, P. T., Allard, P., Haapaniemi, P., Vihinen, M., Smith, C. I., and Hard, T. (1998) Solution structure of the SH3 domain from Bruton's tyrosine kinase. *Biochemistry 37*, 2912–2924.
19. Hyvonen, M., and Saraste, M. (1997) Structure of the PH domain and Btk motif from Bruton's tyrosine kinase: molecular explanations for X-linked agammaglobulinaemia. *EMBO J. 16*, 3396–3404.
20. Mao, C., Zhou, M., and Uckun, F. M. (2001) Crystal structure of Bruton's tyrosine kinase domain suggests a novel pathway for activation and provides insights into the molecular basis of X-linked agammaglobulinemia. *J. Biol. Chem. 276*, 41435–41443.
21. Tzeng, S. R., Lou, Y. C., Pai, M. T., Jain, M. L., and Cheng, J. W. (2000) Solution structure of the human BTK SH3 domain complexed with a proline-rich peptide from p120cbl. *J. Biomol. NMR 16*, 303–312.
22. Marquez, J. A., Smith, C. I., Petoukhov, M. V., Lo Surdo, P., Mattsson, P. T., Knekt, M., Westlund, A., Scheffzek, K., Saraste, M., and Svergun, D. I. (2003) Conformation of full-length Bruton tyrosine kinase (Btk) from synchrotron X-ray solution scattering. *EMBO J. 22*, 4616–4624.
23. Kang, S. W., Wahl, M. I., Chu, J., Kitaura, J., Kawakami, Y., Kato, R. M., Tabuchi, R., Tarakhovsky, A., Kawakami, T., Turck, C. W., Witte, O. N., and Rawlings, D. J. (2001) PKCbeta modulates antigen receptor signaling via regulation of Btk membrane localization. *EMBO J. 20*, 5692–5702.
24. Guo, S., Ferl, G. Z., Deora, R., Riedinger, M., Yin, S., Kerwin, J. L., Loo, J. A., and Witte, O. N. (2004) A phosphorylation site in Bruton's tyrosine kinase selectively regulates B cell calcium signaling efficiency by altering phospholipase C-gamma activation. *Proc. Natl. Acad. Sci. U.S.A. 101*, 14180–14185.
25. Dinh, M., Grunberger, D., Ho, H., Tsing, S. Y., Shaw, D., Lee, S., Barnett, J., Hill, R. J., Swinney, D. C., and Bradshaw, J. M. (2007) Activation mechanism and steady state kinetics of Bruton's tyrosine kinase. *J. Biol. Chem. 282*, 8768–8776.
26. Shaffer, J., and Adams, J. A. (1999) An ATP-linked structural change in protein kinase A precedes phosphoryl transfer under physiological magnesium concentrations. *Biochemistry 38*, 5572–5581.
27. Hashimoto, S., Iwamatsu, A., Ishiai, M., Okawa, K., Yamadori, T., Matsushita, M., Baba, Y., Kishimoto, T., Kurosaki, T., and Tsukada, S. (1999) Identification of the SH2 Domain Binding Protein of Bruton's Tyrosine Kinase as BLNK---Functional Significance of Btk-SH2 Domain in B-Cell Antigen Receptor-Coupled Calcium Signaling. *Blood 94*, 2357–2364.
28. Veillette, A., Caron, L., Fournel, M., and Pawson, T. (1992) Regulation of the enzymatic function of the lymphocyte-specific tyrosine protein kinase p56lck by the non-catalytic SH2 and SH3 domains. *Oncogene 7*, 971–980.
29. Saito, K., Scharenberg, A. M., and Kinet, J. P. (2001) Interaction between the Btk PH domain and phosphatidylinositol-3,4,5-trisphosphate directly regulates Btk. *J. Biol. Chem. 276*, 16201–16206.

30. Segel, I. H. (1975) *Enzyme Kinetics*, John Wiley and Sons Inc., New York.
31. Waas, W. F., and Dalby, K. N. (2003) Physiological Concentrations of Divalent Magnesium Ion Activate the Serine/Threonine Specific Protein Kinase ERK2. *Biochemistry 42*, 2960–2970.
32. Lowry, W. E., Huang, J., Lei, M., Rawlings, D., and Huang, X. Y. (2001) Role of the PHTH module in protein substrate recognition by Bruton's agammaglobulinemia tyrosine kinase. *J. Biol. Chem. 276*, 45276–45281.
33. Joseph, R. E., Min, L., and Andreotti, A. H. (2007) The linker between SH2 and kinase domains positively regulates catalysis of the Tec family kinases. *Biochemistry 46*, 5455–5462.
34. Yamaguchi, H., and Hendrickson, W. A. (1996) Structural basis for activation of human lymphocyte kinase Lck upon tyrosine phosphorylation. *Nature 384*, 484–489.
35. Breitenlechner, C. B., Kairies, N. A., Honold, K., Scheiblich, S., Koll, H., Greiter, E., Koch, S., Schafer, W., Huber, R., and Engh, R. A. (2005) Crystal structures of active SRC kinase domain complexes. *J. Mol. Biol. 353*, 222–231.
36. Brown, K., Long, J. M., Vial, S. C., Dedi, N., Dunster, N. J., Renwick, S. B., Tanner, A. J., Frantz, J. D., Fleming, M. A., and Cheetham, G. M. (2004) Crystal structures of interleukin-2 tyrosine kinase and their implications for the design of selective inhibitors. *J. Biol. Chem. 279*, 18727–18732.
37. Adams, J. A. (2003) Activation loop phosphorylation and catalysis in protein kinases: is there functional evidence for the autoinhibitor model? *Biochemistry 42*, 601–607.
38. Mildvan, A. S., Rosevear, P. R., Fry, D. C., Bramson, H. N., and Kaiser, E. T. (1985) NMR studies of the mechanism of action and regulation of protein kinase. *Curr. Top. Cell. Regul. 27*, 133–144.
39. Sun, G., and Budde, R. J. (1997) Requirement for an additional divalent metal cation to activate protein tyrosine kinases. *Biochemistry 36*, 2139–2146.
40. Nolen, B., Taylor, S., and Ghosh, G. (2004) Regulation of protein kinases; controlling activity through activation segment conformation. *Mol. Cell 15*, 661–675.
41. Pawson, T., Olivier, P., Rozakis-Adcock, M., McGlade, J., and Henkemeyer, M. (1993) Proteins with SH2 and SH3 domains couple receptor tyrosine kinases to intracellular signalling pathways. *Philos. Trans. R. Soc. London, Ser. B 340*, 279–285.
42. Williams, J. C., Weijland, A., Gonfloni, S., Thompson, A., Courtneidge, S. A., Superti-Furga, G., and Wierenga, R. K. (1997) The 2.35 A crystal structure of the inactivated form of chicken Src: a dynamic molecule with multiple regulatory interactions. *J. Mol. Biol. 274*, 757–775.
43. Xu, W., Doshi, A., Lei, M., Eck, M. J., and Harrison, S. C. (1999) Crystal structures of c-Src reveal features of its autoinhibitory mechanism. *Mol. Cell 3*, 629–638.
44. Xu, W., Harrison, S. C., and Eck, M. J. (1997) Three-dimensional structure of the tyrosine kinase c-Src.[see comment]. *Nature 385*, 595–602.
45. Huse, M., and Kuriyan, J. (2002) The conformational plasticity of protein kinases. *Cell 109*, 275–282.
46. Hantschel, O., Nagar, B., Guettler, S., Kretzschmar, J., Dorey, K., Kuriyan, J., and Superti-Furga, G. (2003) A myristoyl/phosphotyrosine switch regulates c-Abl.[see comment]. *Cell 112*, 845–857.
47. Nagar, B., Hantschel, O., Young, M. A., Scheffzek, K., Veach, D., Bornmann, W., Clarkson, B., Superti-Furga, G., and Kuriyan, J. (2003) Structural basis for the autoinhibition of c-Abl tyrosine kinase.[see comment]. *Cell 112*, 859–871.
48. Ogawa, A., Takayama, Y., Sakai, H., Chong, K. T., Takeuchi, S., Nakagawa, A., Nada, S., Okada, M., and Tsukihara, T. (2002) Structure of the carboxyl-terminal Src kinase, Csk. *J. Biol. Chem. 277*, 14351–14354.
49. Sondhi, D., and Cole, P. A. (1999) Domain interactions in protein tyrosine kinase Csk. *Biochemistry 38*, 11147–11155.
50. Sun, G., and Budde, R. J. (1999) Mutations in the N-terminal regulatory region reduce the catalytic activity of Csk, but do not affect its recognition of Src. *Arch. Biochem. Biophys. 367*, 167–172.
51. Lin, X., Ayrapetov, M. K., Lee, S., Parang, K., and Sun, G. (2005) Probing the communication between the regulatory and catalytic domains of a protein tyrosine kinase, Csk. *Biochemistry 44*, 1561–1567.
52. Smith, C. I., Islam, T. C., Mattsson, P. T., Mohamed, A. J., Nore, B. F., and Vihinen, M. (2001) The Tec family of cytoplasmic tyrosine kinases: mammalian Btk, Bmx, Itk, Tec, Txk and homologs in other species. *Bioessays 23*, 436–446.

BI8019756